


Article

Prediction of the Dynamic Stiffness of Resilient Materials using Artificial Neural Network (ANN) Technique

Changhyuk Kim ¹, Jung-Yoon Lee ¹ and Moonhyun Kim ^{2,*}

¹ School of Civil, Architectural Engineering and Landscape Architecture, Sungkyunkwan University, Suwon 16419, Korea; changhyuk@skku.edu (C.K.); jungyoon@skku.edu (J.-Y.L.)

² College of Software, Sungkyunkwan University, Suwon 16419, Korea; mhkim@skku.edu

* Correspondence: mhkim@skku.edu

Received: 6 March 2019; Accepted: 12 March 2019; Published: 14 March 2019



Abstract: High-rise residential buildings are constructed in countries with high population density in response to the need to utilize small development areas. As many high-rise buildings are being constructed, issues of floor impact sound tend to occur in buildings. In general, resilient materials are implemented between the slab and the finishing mortar to control the floor impact sound. Various mechanical properties of resilient materials can affect the floor impact sound. To investigate the impact sound reduction capacity, various experimental tests were conducted. The test results show that the floor impact sound reduction capacity has a close relationship with the dynamic stiffness of resilient materials. A total of six different kinds of resilient materials were loaded under four loading conditions. The test results show that loading time, loading, and material properties influence the change in dynamic stiffness. Artificial neural network (ANN) technique was implemented to obtain the responses between the deflection and dynamic stiffness. Three different algorithms were considered in the ANN models and the trained results were analyzed based on the root mean square error. The feasibility of using the ANN technique was verified with a high and consistent level of accuracy.

Keywords: artificial neural network; data regression; resilient material; long-term load; dynamic stiffness

1. Introduction

In Asian countries, where the population density is very high, high-rise residential buildings are common. The issue of floor impact sound tends to occur in most high-rise buildings. Many countries have set regulations for controlling floor impact sounds [1–3]. Various systems are needed to minimize the floor impact sounds and one of the most effective ways is to use a floating floor system.

Many studies have shown that lightweight and heavyweight impact sounds can be reduced by using resilient materials. Findley [4] developed an empirical and analytical model to evaluate the influence of impact sound transmission on low frequencies. Experimental tests on the response between the floor impact sound reduction and dynamic stiffness showed that as the dynamic stiffness decreases, the lightweight impact sound reduction tends to increase [5]. Measuring the apparent dynamic stiffness is an important procedure for evaluating the impact sound reduction. Kim and Lee [6] conducted an experimental study on the relation between the long-term deflection and dynamic stiffness considering various resilient materials. The creep behavior of polymer materials has been extensively studied in the chemical engineering field [7–9]. However, the objective of the studies was to determine the creep behavior of the polymer material itself. Kim et al. [10] conducted an experimental

study to evaluate the response between the deflection and dynamic stiffness under long-term loading, and proposed an equation to predict the dynamic stiffness.

An artificial neural network (ANN) is a generalized mathematical model that resembles human neural biology. Many ANN techniques have been proposed to predict or classify various data. These techniques are useful to predict unknown output data, depending on various input values [11,12]. Many studies have presented the feasibility of using ANNs in civil and other engineering areas with good results. Yang et al. [13] researched an optimum mixture design of reactive powder concrete based on an ANN to establish the relationship between the design parameters and properties of reactive powder concrete. The proposed ANN model can be used for optimum design in different regions. Rafiei et al. [14] reported computational intelligence techniques to estimate concrete properties using previously collected data. Linear and nonlinear regression were considered as statistical techniques. The backpropagation neural network and self-organization feature map were used as neural network techniques. Sebaaly et al. [15] presented an automatic mix design process to optimize asphalt mix constituents. A simple multilayer perceptron structure was developed using Marshall mix design data. Singh et al. [16] investigated the effect of using marble slurry to partially replace cement by weight in concrete. A compressive strength prediction model was developed to verify the experimentally evaluated 28-day compressive strength. They reported that the proposed model would be useful in predicting the 28-day compressive strength for concrete incorporating marble slurry. Azimi-Pour and Eskandari-Naddaf [17] proposed ANN and genetic expression programming models to predict the effect of nano silica and micro silica on cement mortar properties. The ANN model was applied to experimental results to verify the performance of the cement mortar. The ANN model was reported to be an alternative approach for evaluation of the silica effect in cement mortar. Shi et al. [18] introduced the prediction of mechanical properties of engineered cementitious composite (ECC) using ANN technique. ANN models were developed for ECC reinforced with polyvinyl alcohol fiber, and experimental data from other researchers were used as a training set. The predicted results showed excellent consistency with the test results.

Various ANN models were proposed to estimate the strength of concrete members. Soltani et al. [19] studied different input parameters on Interface shear Transfer capacity using artificial neural network models that produce consistent levels of accuracy. Lee and Lee [20] introduced a theoretical ANN model to predict the shear strength of fiber reinforced polymer (FRP) reinforced concrete members. The developed comparisons between the developed ANN model and experimental data indicated that the ANN model resulted in better accuracy than other existing design equations. Cascardi et al. [21] presented an ANN model to predict the strength of FRP confined concrete. Extensive test data were considered to define the variables of the proposed equations. The proposed ANN model was adapted for the FRP confined concrete design, and guaranteed improved accuracy. Elshafey et al. [22] used an ANN model to predict the punching shear strength of slab-column connections based on 244 test data. Two simplified punching shear equations were developed in the study. Morfidis and Kostinakis [23] predicted the seismic damage state of reinforced concrete buildings based on ANN investigation using multilayer feedforward perceptron networks. The ANN model can be used to reliably approach the seismic damage state of buildings. Pathirage et al. [24] proposed an autoencoder-based framework that can support deep ANN. To verify the accuracy and efficiency of the proposed framework, experimental studies on steel frame structures were conducted. Sollazzo et al. [25] introduced an ANN to estimate the structural performance of asphalt pavements. Several significant input parameters were considered in the analysis. The authors trained three different ANNs to analyze datasets. Androjić and Dolaček-Alduk [26] provided an ANN model with the objective of predicting the consumption of natural gas during asphalt production. Tosun et al. [27] used linear regression and artificial neural network modeling to predict engine performance. It was reported that the use of ANN was more accurate than the use of linear regression modeling.

In addition to the various studies mentioned above, various ANN models have been proposed to predict the tensile and compressive strength of concrete [28–32]. The proposed models considered

various input data and showed good precision and accuracy compared with the experimental results. Therefore, the applicability of ANN models can be verified based on diverse studies.

Many previous studies on resilient materials have been conducted based on experiments. However, to the best of our knowledge, the behavior of resilient material using ANN modeling has not been studied. In this paper, a prediction of the relation between the deflection response and the dynamic stiffness of the resilient materials was investigated using ANN models. Kim et al. [10] proposed an empirical equation to predict the responses between long-term deflection and dynamic stiffness. The proposed equation can predict the trend of the responses. However, since only four variables were considered in the equation, there was a limit to the accuracy. Therefore, in this paper, mathematical approaches based on the universal approximation theorem were conducted to predict the dynamic stiffness of resilient materials. Three different ANN models with seven variables were proposed, and the results were compared.

2. Experimental Study

2.1. Test Specimens

Table 1 shows the six resilient materials that were chosen to investigate the response between long-term deflection and dynamic stiffness of resilient materials. These materials are generally applied to most construction of Korean residential buildings, and have various material properties.

Figure 1 shows the bottom shape and cross-section of the specimens. The resilient materials were manufactured in corrugated, embossed, and flat shapes. Table 1 shows the nomenclature and the material properties of the resilient materials. Material type, density and the bottom shape of the specimens were represented by the first, second, and third nomenclature groups, respectively. According to ISO 20392, the dimensions of the specimen were 150 mm × 150 mm × 30 mm, and four different weights (40, 80, 250, and 500 N) of loading plates were placed on each specimen.

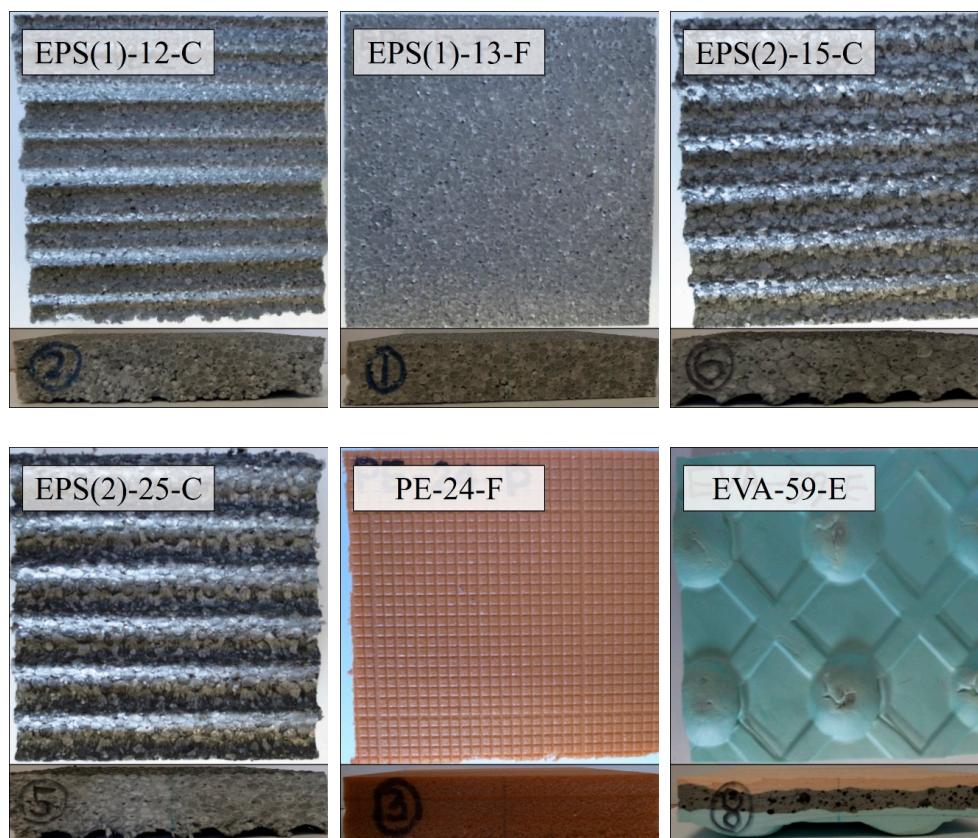


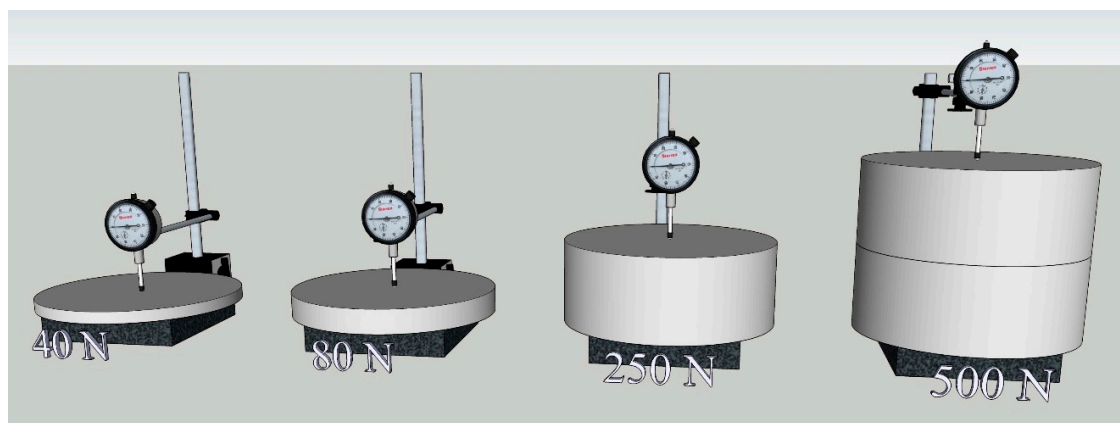
Figure 1. Bottom shape and cross-section of the six resilient materials.

Table 1. Details of specimens.

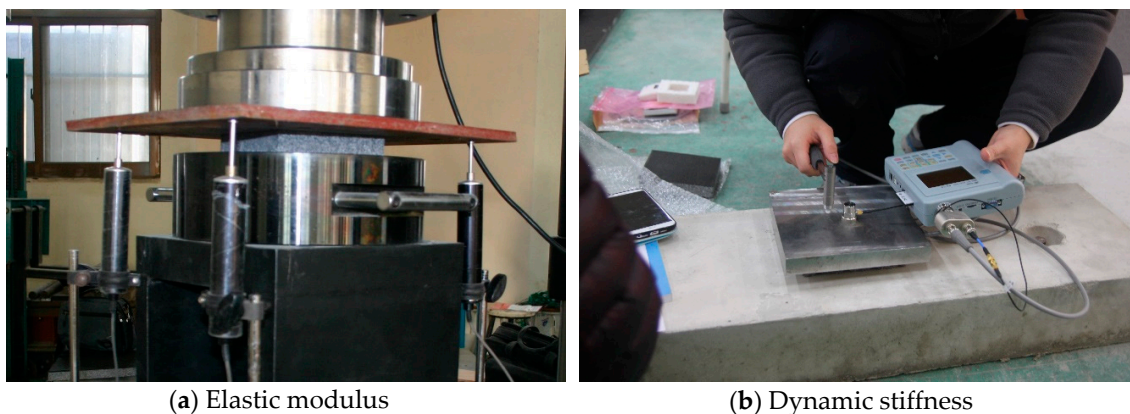
Specimen	Material	Density (kg/m ³)	Bottom Shape	Elastic Modulus (MPa)
EPS(1)-12-C	Ethylene Polystyrene	12.1	Corrugated	0.15
EPS(1)-13-F	Type 1	13.2	Flat	0.23
EPS(2)-15-C	Ethylene Polystyrene	15.4	Corrugated	0.11
EPS(2)-25-C	Type 2	25.5	Corrugated	0.12
PE-24-F	Polystyrene	24.0	Flat	0.16
EVA-59-E	Ethylene Vinyl Acetate	59.3	Embossed	0.11

2.2. Test Measurements

Figure 2 shows the experimental apparatus for measuring the deflection of the resilient materials. The weights of the loading plate considered in this experimental study were (40, 80, 250, and 500) N. Four loading plates were used to reflect the various loading conditions in the actual building. The stresses correspond to loads of 250 and 500 N were 0.011 and 0.022 MPa, respectively. These stresses can simulate the stresses caused by a refrigerator or piano in buildings. Permanent loads can be reflected by using 40 and 80 N loadings. A dial gauge with an accuracy of 1/100 mm was used to record the long-term deflection of the resilient materials. The dial gauges were placed on the center of the loading plates using a magnetic base. All specimens were placed on a sturdy shelf.

**Figure 2.** Test setup for deflection of the resilient materials.

The elastic modulus of the test specimen was measured using a Universal Testing Machine (UTM) (Figure 3a), and three specimens were measured for each material. The dynamic stiffness was recorded based on the Korean Standard F 2868 [33] and a pulse excitation method was used in this study (Figure 3b).

**Figure 3.** Measurement of elastic modulus and dynamic stiffness.

3. Artificial Neural Network (ANN)

We formulated the training data set, $S = \{(x^1, y^1), (x^2, y^2), \dots, (x^n, y^n)\}$, where x^i denotes the i th input feature vector, and y^i denotes the i th output value. In this paper, a feature vector consists of the 7 variables and the y is measured dynamic stiffness for that feature vector. In addition to MLP regression as a typical ANN model for prediction, we also applied the distance weighted k-nn method and the regression tree method which are known to be effective for prediction of nonlinear function.

3.1. Distance-Weighted k-nn Regression

Firstly, we applied distance-weighted k-nn regression algorithm.

This finds the k nearest feature vectors $x^i, i = 1, \dots, k$ of the current input feature vector x^q from the stored training data set, and computes the distance between the current input feature vector x^q and each nearest feature vector x^i :

$$d(x^q, x^i) = \|x^q - x^i\|, i = 1, \dots, k \tag{1}$$

The weight for each nearest feature vector is computed using distance:

$$w_i = \frac{1}{d(x^q, x^i)}, i = 1, \dots, k \tag{2}$$

Then it predicts the output $F(x^q)$ using the weighted average, as follows:

$$F(x^q) = \frac{\sum_{i=1}^k w_i y^i}{\sum_{i=1}^k w_i} \tag{3}$$

where y^i is the corresponding output of the i^{th} nearest feature vector x^i .

3.2. Regression Tree

The regression tree algorithm constructs a decision tree from a provided training set S . After constructing a tree in the learning phase, it predicts the output $F(x^q)$ of current input vector x^q by searching the tree. Starting from the root node, it selects a child node depending on the value of the feature specified at each node. The leaf node shows an estimated value of the function, i.e., $F(x^q)$. We built the regression tree as follows:

Step 1. Initially, the mean of the output value for set S is computed as:

$$m = \frac{1}{n} \sum_{y^j \in S} y^j \tag{4}$$

Then the variance is computed as:

$$\text{Var} = \frac{1}{|S|} \sum_{y^i \in S} (y^i - m)^2 \tag{5}$$

Set S is made the root node of the regression tree.

Step 2. For each feature $x_i, i = 1, \dots, d$, search all possible binary splits $\{S_1^i, S_2^i\}$ from set S of the parent node.

Binary split using the i th feature is the partition of S , as follows;

$$S = S_1^i \cup S_2^i, S_1^i = \{(x^j, y^j) \mid l_1 < x_i^j \leq u_1\}, S_2^i = \{(x^j, y^j) \mid l_2 < x_i^j \leq u_2\}, \text{ and } u_1 = l_2 \tag{6}$$

and compute the mean m_1^i, m_2^i for two split sets S_1^i, S_2^i , respectively.

$$m_k^i = \frac{1}{n_k^i} \sum_{y^j \in S_k^i} y^j, k = 1, 2 \tag{7}$$

where n_k^i is the number of data in set S_k^i .

The variance for split is computed as:

$$\text{Var2} = \frac{1}{|S_1^i|} \sum_{y^i \in S_1^i} (y^i - m_1^i)^2 + \frac{1}{|S_2^i|} \sum_{y^i \in S_2^i} (y^i - m_2^i)^2 \tag{8}$$

Select a binary split that has minimum variance from all possible binary splits using every feature. Compute the decrease of variance from the parent node.

If the decrease in variance is less than the predefined threshold α , then stop. Otherwise, accept that split, and create two child nodes, where each node corresponds to S_1^i, S_2^i , respectively.

Step 3. For each child node, go to step 2.

3.3. Multiple Layer Perceptron Regression

We applied multiple layer perceptron regression (MLP Regression) algorithm (Figure 4). The number of hidden layers is assigned as 1. The number of hidden units for each layer is changed as a parameter during experimentation.

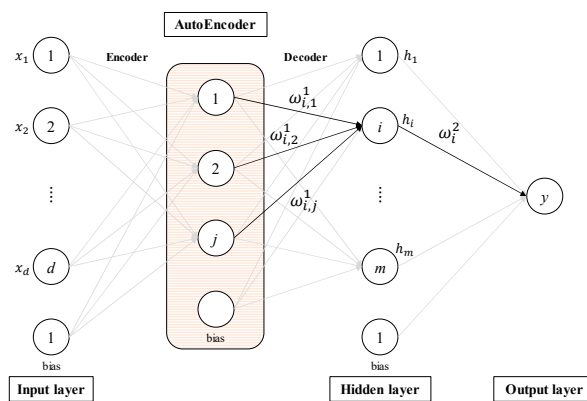


Figure 4. Schematic diagram of MLP regression.

At each layer, we first compute the total input z to each unit, which is a weighted sum of the outputs of the units in the layer below. For the first hidden layer, the input z_i for the i th hidden unit,

$$z_i = \sum_{j=1}^{d+1} w_{ij}^1 x_j \tag{9}$$

where w_{ij}^1 is the connection weight from the j th input unit to the i th hidden unit, and d is the number of input units. For the output unit, the input is computed as:

$$z_o = \sum_{j=1}^{m+1} w_j^2 h_j \tag{10}$$

where, w_j^2 is the connection weight from the j th hidden unit of the hidden layer to the output unit, h_j is the output of the j th hidden unit of the hidden layer, and m is the number of hidden units of the hidden layer. For the input layer and hidden layers, a unit with output 1 is added to include a bias term.

Then a non-linear function $f^h(\cdot)$ is applied to z_i to get the output of the hidden unit. The activation function used is the sigmoid function, i.e.,

$$f^h(z_i) = \frac{1}{1 + e^{-z_i}} \tag{11}$$

The activation function for the output unit is a linear function, i.e.,

$$f^o(z_o) = z_o \tag{12}$$

Output $f^o(z_o)$ is the predicted output $F(x^o)$ of the current input feature vector x^o .

For the input, we used an auto encoder to transform the input feature vector to a new feature vector using unsupervised learning. The autoencoder is a 2-layer perceptron with one hidden layer. The autoencoder learns effective representation of the input data from the provided unlabeled training data, and it tries to generate output so that it is equal to input. The used cost function is:

$$J(\mathbf{w}) = \frac{1}{n} \sum_{i=1}^n \frac{1}{2} h(\mathbf{w}, x^i) - x^{i2} + \frac{\alpha}{2} \left\{ \sum_{i=1}^d \sum_{j=1}^m (w_{ji}^1)^2 + \sum_{i=1}^m \sum_{j=1}^d (w_{ji}^2)^2 \right\} \tag{13}$$

where m is the number of hidden units, $h(\mathbf{w}, x^i)$ is the output of autoencoder for x^i , and \mathbf{w} is the weight vector of the encoder and decoder. The first term of $J(\mathbf{w})$ is an average sum-of-squares error term. The second term is a regularization term (also called a weight decay term) to decrease the magnitude of the weights. The α is called the weight decay parameter to control the relative importance between the two terms. After learning, the output value of the hidden layer $\mathbf{h} = [h_1, \dots, h_m]^T$ becomes a transformed vector. This transformed vector will be used as a new input vector for MLP regression for each data.

4. Results and Discussion

4.1. Empirical Equation and ANN Algorithms

This section compares the relation between the deflection and dynamic stiffness based on the test results to the equation proposed by Kim et al. [10], and the artificial neural network modeling using three different data regression algorithms. Equation (14) shows the proposed equation. The proposed equation uses the dynamic stiffness after 30 min after loading, the applied load, the elastic modulus, and the material coefficients. However, the ANN system considers the following seven attributes for the training data set: applied load, density, elastic modulus at early loading stage, dynamic stiffness after 30-min loading, shape, deflection, and dynamic stiffness.

$$DS = DS_{30} + \frac{3}{P} e^{(\frac{\Delta C_1}{3} - C_2 \frac{P}{E})} \tag{14}$$

where DS is the dynamic stiffness (MN/m^3), DS_{30} is the dynamic stiffness 30 min after loading (MN/m^3), P is the applied load (N), E is the elastic modulus (MPa), and Δ is the deflection (mm).

Various nearest feature vectors of distance-weighted k-nn, tree depth and nodes were tested to obtain the minimum Root Mean Squared Error (RMSE) of k-nn regression, regression tree, and MLP Regression, respectively. Figure 5 plots the test results of the three data regression algorithms. The X-axis and Y-axis represent the number of variables and the calculated RMSE results, respectively. In the case of the k-nn regression algorithm, the RMSE was the smallest when the value of weighted k-nn was 3. In the case of the regression tree and MLP regression, the RMSE was the smallest when the tree depth was 10 and the number of nodes was 8, respectively.

Table 2 shows the correlation coefficient, Root Mean Square Error (RMSE), Relative Absolute Error (RAE), and Root Relative Square Error (RRSE) of the algorithms used in this study. Each error can be calculated using the following equations.

$$RMSE = \sqrt{\frac{1}{n} \sum_{i=1}^n (p_i - y_i)^2} \tag{15}$$

$$RAE = \frac{\sum_{i=1}^n |p_i - y_i|}{\sum_{i=1}^n |\bar{p}_i - y_i|} \tag{16}$$

$$RRSE = \sqrt{\frac{\sum_{i=1}^n (p_i - y_i)^2}{\sum_{i=1}^n (\bar{p}_i - y_i)^2}} \tag{17}$$

where n is the number of data set, p_i is the predicted value, y_i is the actual value, \bar{p}_i is the mean value.

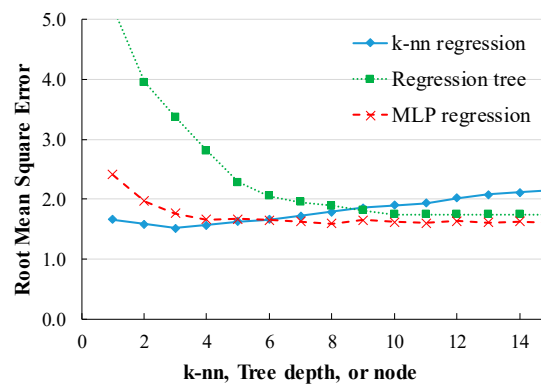


Figure 5. RMSE comparison of the three algorithms.

The correlation coefficient and the errors of the proposed equation by Kim et al. [10] were also calculated for comparison. Since the average correlation coefficient of the three algorithms was 0.9843, the three models are confirmed to well reflect the data of the training set. The correlation coefficient of the ANN models was about 9.5% more than that of the proposed equation by Kim et al. Also, when the ANN models were used, the RMSE decreased by 54.4% and the relative errors decreased by an average of 92.0%. Table 2 confirms that when the ANN algorithms were used, the accuracy was significantly improved Tables 3 and A1 show the calculated weight values between the (input layer and hidden layer) and (hidden layer and output) for dynamic stiffness prediction.

Table 2. Error comparison between the ANN algorithms.

Algorithm	Correlation Coefficient	Root Mean Square Error	Relative Absolute Error (%)	Root Relative Square Error (%)
k-nn regression	0.9864	1.5221	12.2242	16.5721
Regression tree	0.9817	1.7481	16.0049	19.0322
MLP Regression	0.9848	1.5931	13.9954	17.3445
Kim et al. [10]	0.8992	3.5529	195.5806	198.8626

Table 3. Weights of the hidden layer (ω_i^2).

	1	2	3	4	5	6	7	8
ω_i^2	-2.533	-4.174	-2.358	-6.918	1.297	2.209	5.622	-1.997

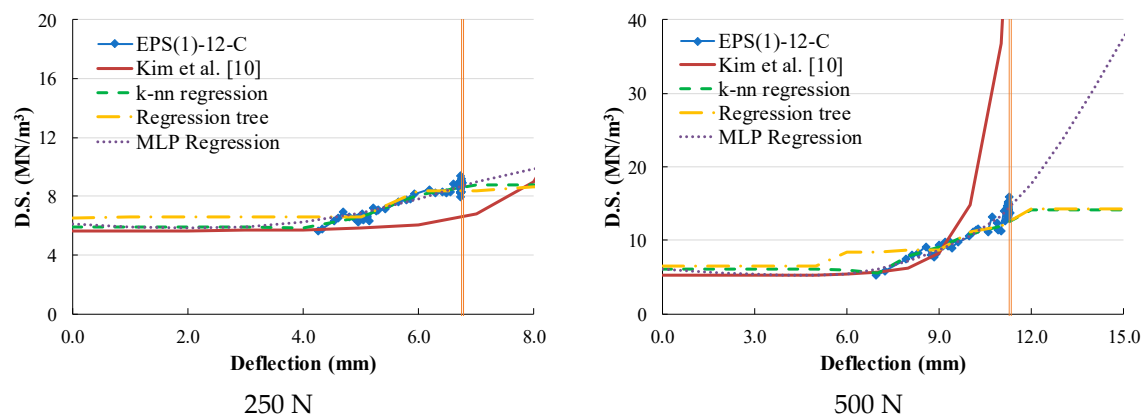
4.2. Test Results and Comparison

Figure 6 compares the responses for the test results, the proposed equation by Kim et al. [10], and the three different models. The 250 and 500 N loading plates were applied to the specimens. Figure A1 of the Appendix shows additional comparison plots under (40 and 80) N loadings. The x - and y -axes represent the deflection of the specimens and the dynamic stiffness, respectively. The solid curves with markers (blue) and the solid curves (red) indicate the test results and the dynamic stiffness calculated using the equation, respectively. The three different types of dashed curves represent the

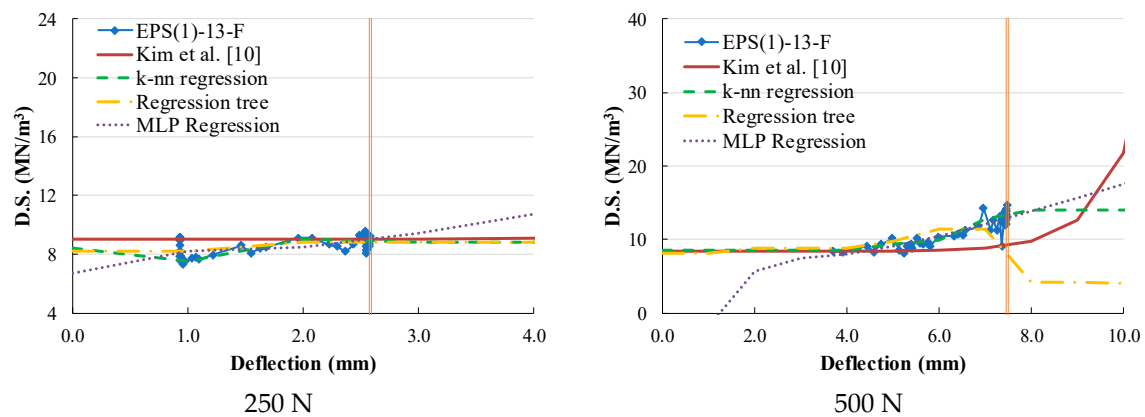
dynamic stiffness predicted using the three ANN algorithms. The vertical line in the plots represents the maximum deflection of the resilient materials under each loading. The deflection was measured for more than 500 days and the load-deflection responses of the specimens were reported by Kim et al. [10]. The vertical line implies the practical maximum deflection of each material.

In most cases, the regression data using the algorithms predicts well the test results. Reasonable data regression among the actual test data was observed in the ANN system using the k-nn regression and regression tree algorithms. However, the regression models could not predict the dynamic stiffness-deflection responses outside of the actual data range. These algorithms were effective only within the actual test data range. MLP Regression more reasonably predicted the test data than the proposed equation in most cases and could predict the deflection dependent dynamic stiffness outside the measured test data. The data regression tendency of these ANN systems was similar in all the specimens.

For example, in the case of EPS(2)-15-C (Figure 5c), the maximum deflection of specimens under (250 and 500) N loading was (10.34 and 17.21) mm, respectively. The three ANN models well predicted the dynamic stiffness prior to reaching the maximum deflection. However, k-nn regression and regression tree algorithms could not track the dynamic stiffness trend after the final deflection, and tended to converge to the final recorded dynamic stiffness. Regardless of the deflection increase, the predicted dynamic stiffness was about (8.34 and 8.10) MN/m³ under (250 and 500) N loading, respectively. On the other hand, MLP regression well inferred the trend of data and showed a similar tendency to the proposed equation. The step-wise prediction responses were monitored in PE-24-F (Figure 6e) when k-nn and regression tree algorithms were applied. This shape is due to the sparsely measured test data in which caused by a significant increase of deflection during the test. However, the continuous curve response was obtained when MLP regression was used.



(a) EPS(1)-12-C



(b) EPS(1)-13-F

Figure 6. Cont.

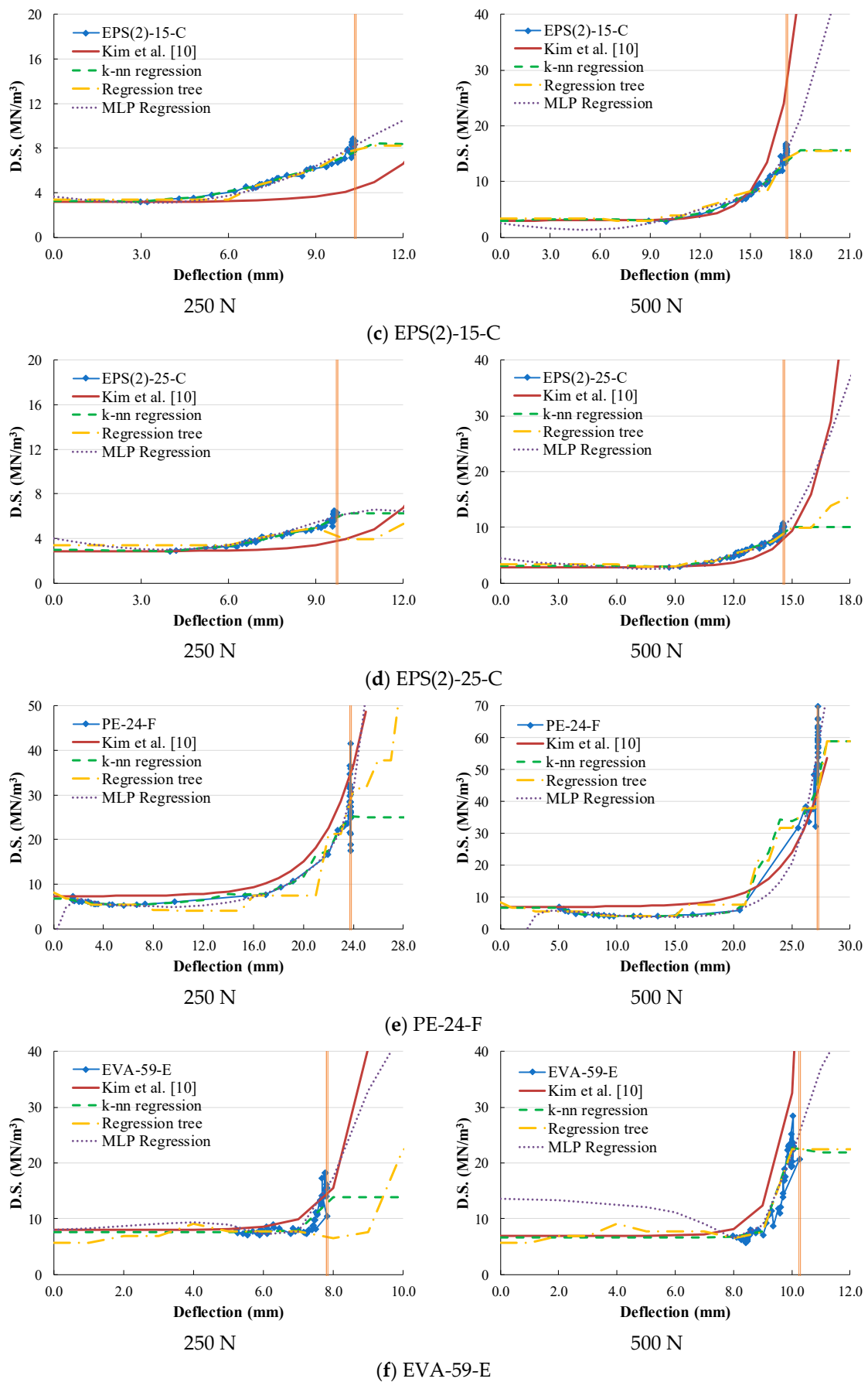


Figure 6. Dynamic stiffness comparisons between the test results and the equation for 250 N and 500 N.

5. Conclusions

Understanding dynamic stiffness behavior is important, since floor impact sound is affected by the dynamic stiffness of resilient materials. The objective of this research was to verify the response between the dynamic stiffness and deflection based on artificial neural network technique. In the previously proposed prediction equation, only four variables were considered; however, 7 mechanical properties of resilient materials were considered to develop ANN algorithms. Therefore, the relationship between deflection and dynamic stiffness could be predicted with higher accuracy.

Three different ANN algorithms were proposed and compared based on RMSE. The correlation coefficient of the dynamic stiffness-deflection relation of the previous equation was only 0.8992; however, when ANN modeling was used, the correlation coefficient increased to an average of 0.9843. When the ANN algorithms were utilized an average of 9.5% of increased correlation coefficient was obtained. In addition, it was confirmed that the values of RMSE, RAE, and RRSE were significantly reduced. RMSE showed an average 54.4% reduction compared to the equation of Kim et al., while RAE and RRSE decreased by 92.8% and 91.1%, respectively.

When the behavior of the resilient material was analyzed using k-nn regression and regression tree algorithms, the prediction curve was greatly affected by the distribution of input data. However, it was verified that when MLP Regression algorithm was applied, the response between dynamic stiffness and deflection was well predicted. Accurate prediction of dynamic stiffness can be obtained when the proposed algorithm was provided, and thereby the ANN technique is applicable to systems for analyzing the behavior of resilient materials.

Author Contributions: Conceptualization, C.K. and M.K.; Methodology, M.K.; Software, C.K.; Validation, C.K.; Formal Analysis, C.K.; Investigation, M.K.; Resources, J.-Y.L.; Data Curation, J.-Y.L. and C.K.; Writing—Original Draft Preparation, C.K.; Writing—Review & Editing, M.K.; Visualization, C.K.; Supervision, M.K.; Project Administration, C.K.; Funding Acquisition, C.K.

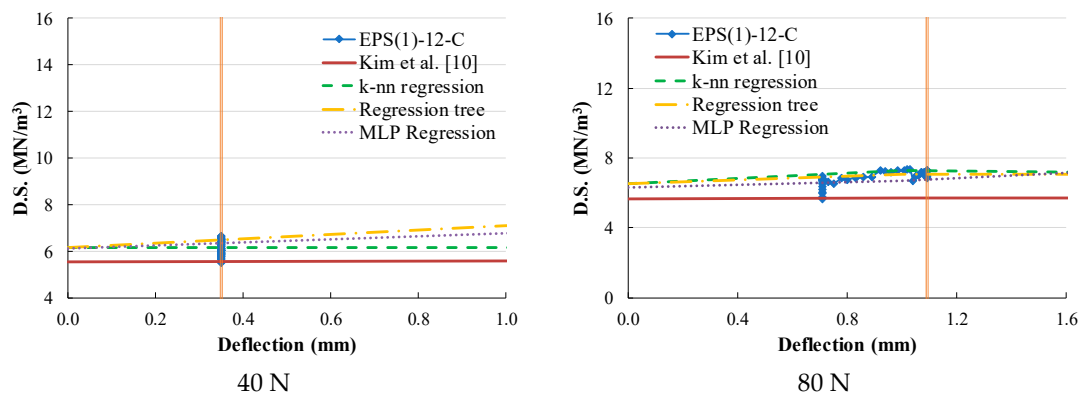
Funding: This research was supported by the Basic Science Research Program through the National Research Foundation of Korea (NRF) funded by the Ministry of Education (NRF-2016R1A6A3A11931420).

Conflicts of Interest: The authors declare no conflict of interest. The funders had no role in the design of the study; in the collection, analyses, or interpretation of data; in the writing of the manuscript, or in the decision to publish the results.

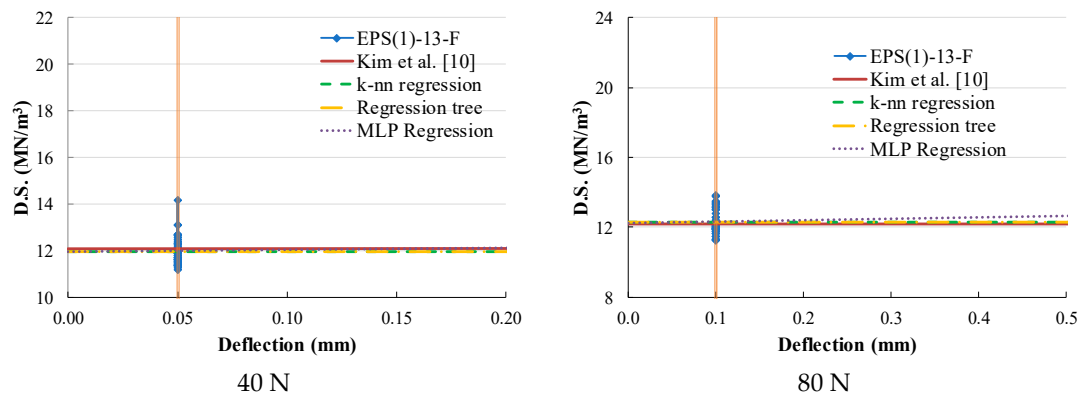
Appendix A

Table A1. Weights of the hidden layer (ω_{ij}^1).

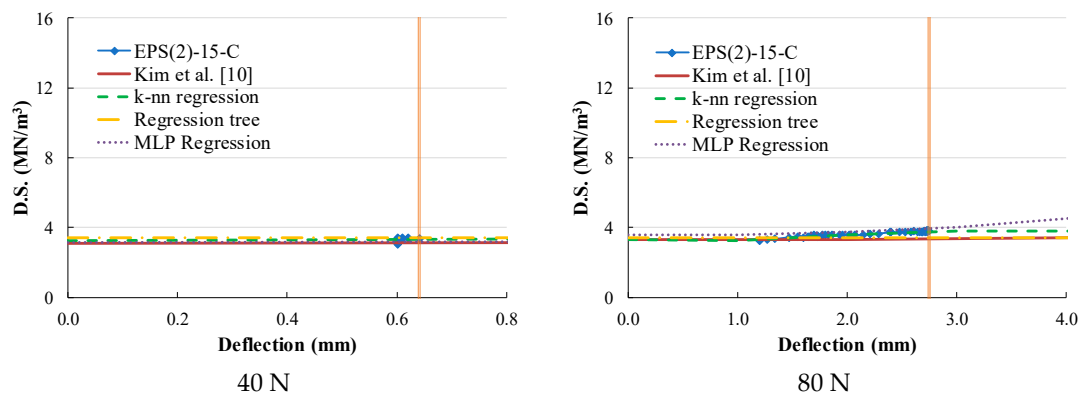
<i>j</i> \ <i>i</i>	1	2	3	4	5	6	7	8
1	1.254	1.025	2.345	−6.354	0.363	2.105	2.761	−0.768
2	−0.048	0.058	0.548	0.051	−0.446	0.109	1.602	0.265
3	−0.628	−0.456	−2.975	3.993	−0.234	−0.698	−3.150	−0.755
4	0.613	2.451	−1.618	−0.527	−0.356	−0.257	−1.823	0.979
5	0.750	1.032	2.012	0.325	−0.286	1.033	3.876	0.874
6	0.347	−0.571	0.425	−0.778	1.103	−0.525	0.314	0.292
7	−1.091	−0.834	0.658	0.667	0.490	0.020	−1.521	−0.009
8	0.428	1.027	−0.986	−3.075	−0.350	−1.113	−2.211	−0.104
9	0.357	−1.621	−0.111	0.162	0.198	−1.188	0.716	0.113
10	0.299	−0.141	−2.049	3.991	−0.962	−1.069	−0.742	−0.064
11	−1.008	1.494	0.285	1.739	−0.106	0.201	0.105	0.111
12	−0.783	−1.423	0.136	−0.618	0.482	0.128	1.975	−0.637
13	0.005	−0.130	0.883	−1.746	0.063	0.104	0.262	−0.453
14	0.454	0.000	0.314	−4.021	0.574	−0.237	2.173	0.262



(a) EPS(1)-12-C



(b) EPS(1)-13-F



(c) EPS(2)-15-C

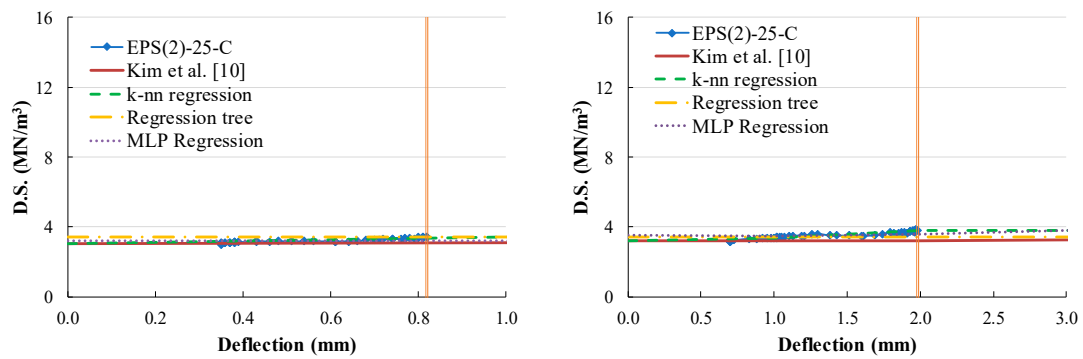


Figure A1. Cont.

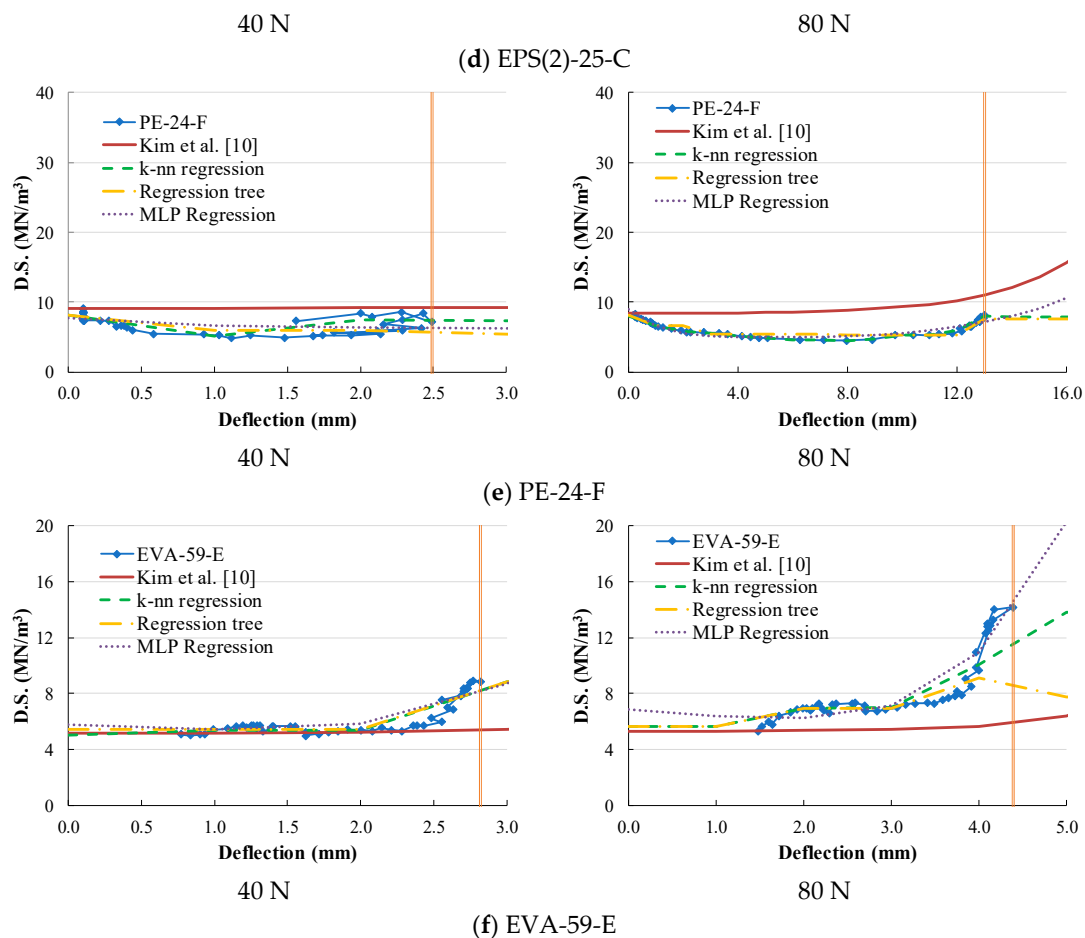


Figure A1. Dynamic stiffness comparisons between the test results and the equation for 40 N and 80 N.

References

- Lee, B.-S.; Jun, M.-H.; Lee, J.-Y. Influencing Factors of the Deflection of Floor Sound Insulation System. *J. Archit. Inst. Korea* **2013**, *29*, 37–44.
- Environmental Quality Standards for Noise. Available online: <https://www.env.go.jp/en/air/noise/noise.html> (accessed on 3 March 2019).
- ACT Parliamentary Counsel. *Environment Protection Act 1997*; A1997-92; ACT Legislation Register: Canberra, ACT, Australia, 1997.
- Findley, W.N. Creep Characteristics of Plastics. In *Proceedings of the Symposium on Plastics*; American Society of Testing and Materials: West Conshohoken, PA, USA, 1994.
- Kim, K.-W.; Jeong, G.-C.; Sohn, J.-Y. Correlation between Dynamic Stiffness of Resilient Materials and Lightweight Floor Impact Sound Reduction Level. *Korean Soc. Noise Vib. Eng.* **2008**, *18*, 886–895.
- Kim, J.; Lee, J.-Y. Evaluation of Long-term Deflection and Dynamic Elastic Modulus of Floor Damping Materials Used in Apartment Buildings. *J. Archit. Inst. Korea* **2014**, *30*, 29–36.
- Gnip, I.Y.; Vaitkus, S.; Keršulis, V.; Vėjelis, S. Analytical description of the creep of expanded polystyrene (EPS) under long-term compressive loading. *Polym. Test.* **2011**, *30*, 493–500. [[CrossRef](#)]
- Raghavan, J.; Meshii, M. Creep of Polymer Composites. *Compos. Sci. Technol.* **1998**, *57*, 1673–1688. [[CrossRef](#)]
- Barbero, E.J. Prediction of Long-term Creep of Composites from Doubly-shifted Polymer Creep Data. *J. Compos. Mater.* **2009**, *43*, 2109–2124. [[CrossRef](#)]
- Kim, C.; Hong, Y.-K.; Lee, J.-Y. Long-term dynamic stiffness of resilient materials in floating floor systems. *Constr. Build. Mater.* **2017**, *133*, 27–38. [[CrossRef](#)]
- Taherdangkoo, R.; Taherdangkoo, M. Application of hybrid neural particle swarm optimisation algorithm to predict solubility of carbon dioxide in blended aqueous amine-based solvents. *Int. J. Softw. Eng. Technol. Appl.* **2015**, *1*, 290–307. [[CrossRef](#)]

12. Taherdangkoo, R.; Taherdangkoo, M. Modified stem cells algorithm-based neural network applied to bottom hole circulating pressure in underbalanced drilling. *Int. J. Pet. Eng.* **2015**, *1*, 178–188. [[CrossRef](#)]
13. Ji, T.; Yang, Y.; Fu, M.Y.; Chen, B.C.; Wu, H.C. Optimum design of reactive powder concrete mixture proportion based on artificial neural and harmony search algorithm. *ACI Mater. J.* **2017**, *114*, 41–47. [[CrossRef](#)]
14. Rafiei, M.H.; Khushefati, W.H.; Demirboga, R.; Adeli, H. Neural network, machine learning, and evolutionary approaches for concrete material characterization. *ACI Mater. J.* **2016**, *113*, 781–789. [[CrossRef](#)]
15. Sebaaly, H.; Varma, S.; Maina, J.W. Optimizing asphalt mix design process using artificial neural network and genetic algorithm. *Constr. Build. Mater.* **2018**, *168*, 660–670. [[CrossRef](#)]
16. Singh, M.; Srivastava, A.; Bhunia, D. An investigation on effect of partial replacement of cement by waste marble slurry. *Constr. Build. Mater.* **2017**, *134*, 471–488. [[CrossRef](#)]
17. Azimi-Pour, M.; Eskandari-Naddaf, H. ANN and GEP prediction for simultaneous effect of nano and micro silica on the compressive and flexural strength of cement mortar. *Constr. Build. Mater.* **2018**, *189*, 978–992. [[CrossRef](#)]
18. Shi, L.; Lin, S.T.K.; Lu, Y.; Ye, L.; Zhang, Y.X. Artificial neural network based mechanical and electrical property prediction of engineered cementitious composites. *Constr. Build. Mater.* **2018**, *174*, 667–674. [[CrossRef](#)]
19. Soltani, M.; Ross, B.E.; Khademi, A. A Statistical Approach to Refine Design Codes for Interface Shear Transfer in Reinforced Concrete Members. *ACI Struct. J.* **2018**, *115*, 1341–1352. [[CrossRef](#)]
20. Lee, S.; Lee, C. Prediction of shear strength of FRP-reinforced concrete flexural members without stirrups using artificial neural networks. *Eng. Struct.* **2014**, *61*, 99–112. [[CrossRef](#)]
21. Cascardi, A.; Micelli, F.; Aiello, M.A. An Artificial Neural Networks model for the prediction of the compressive strength of FRP-confined concrete circular columns. *Eng. Struct.* **2017**, *140*, 199–208. [[CrossRef](#)]
22. Elshafey, A.A.; Rizk, E.; Marzouk, H.; Haddara, M.R. Prediction of punching shear strength of two-way slabs. *Eng. Struct.* **2011**, *33*, 1742–1753. [[CrossRef](#)]
23. Morfidis, K.; Kostinakis, K. Approaches to the rapid seismic damage prediction of r/c buildings using artificial neural networks. *Eng. Struct.* **2018**, *165*, 120–141. [[CrossRef](#)]
24. Pathirage, C.S.N.; Li, J.; Li, L.; Hao, H.; Liu, W.; Ni, P. Structural damage identification based on autoencoder neural networks and deep learning. *Eng. Struct.* **2018**, *172*, 13–28. [[CrossRef](#)]
25. Sollazzo, G.; Fwa, T.F.; Bosurgi, G. An ANN model to correlate roughness and structural performance in asphalt pavements. *Constr. Build. Mater.* **2017**, *134*, 684–693. [[CrossRef](#)]
26. Androjić, I.; Dolaček-Alduk, Z. Artificial neural network model for forecasting energy consumption in hot mix asphalt (HMA) production. *Constr. Build. Mater.* **2018**, *170*, 424–432. [[CrossRef](#)]
27. Tosun, E.; Aydin, K.; Bilgili, M. Comparison of linear regression and artificial neural network model of a diesel engine fueled with biodiesel-alcohol mixtures. *Alexandria Eng. J.* **2016**, *55*, 3081–3089. [[CrossRef](#)]
28. Bui, D.K.; Nguyen, T.; Chou, J.S.; Nguyen-Xuan, H.; Ngo, T.D. A modified firefly algorithm-artificial neural network expert system for predicting compressive and tensile strength of high-performance concrete. *Constr. Build. Mater.* **2018**, *180*, 320–333. [[CrossRef](#)]
29. Yu, Y.; Li, W.; Li, J.; Nguyen, T.N. A novel optimised self-learning method for compressive strength prediction of high performance concrete. *Constr. Build. Mater.* **2018**, *184*, 229–247. [[CrossRef](#)]
30. Rebouh, R.; Boukhatem, B.; Ghrici, M.; Tagnit-Hamou, A. A practical hybrid NNGA system for predicting the compressive strength of concrete containing natural pozzolan using an evolutionary structure. *Constr. Build. Mater.* **2017**, *149*, 778–789. [[CrossRef](#)]
31. Eskandari-Naddaf, H.; Kazemi, R. ANN prediction of cement mortar compressive strength, influence of cement strength class. *Constr. Build. Mater.* **2017**, *138*, 1–11. [[CrossRef](#)]
32. Getahun, M.A.; Shitote, S.M.; Abiero Gariy, Z.C. Artificial neural network based modelling approach for strength prediction of concrete incorporating agricultural and construction wastes. *Constr. Build. Mater.* **2018**, *190*, 517–525. [[CrossRef](#)]
33. KS F 2868 Determination of Dynamic Stiffness of Materials Used Under Floating Floors in Dwellings; Korean Standards Association: Seoul, Korea, 2003; KS F 2868:2003.

